Anal. Chem. **2002,** *74,* 4235−4249

High-Efficiency Nanoscale Liquid Chromatography Coupled On-Line with Mass Spectrometry Using Nanoelectrospray Ionization for Proteomics

Yufeng Shen, Rui Zhao, Scott J. Berger, Gordon A. Anderson, Nestor Rodriguez, and Richard D. Smith*

Environmental Molecular Sciences Laboratory, Pacific Northwest National Laboratory, Richland, Washington 99352

We describe high-efficiency (peak capacities of ∼10^3) nanoscale (using column inner diameters down to 15 μm) liquid chromatography (nanoLC)/low flow rate electrospray (nanoESI) mass spectrometry (MS) for the sensitive analysis of complex global cellular protein enzymatic digests (i.e., proteomics). Using a liquid slurry packing method with carefully selected packing solvents, 87-cm-length capillaries having inner diameters of 14.9−74.5 μm were successfully packed with 3-μm C18-bonded porous (300-Å pores) silica particles at a pressure of 18 000 psi. With a mobile-phase delivery pressure of 10 000 psi, these packed capillaries provided mobile-phase flow rates as low as ∼20 nL/min at LC linear velocities of ∼0.2 cm/s, which is near optimal for separation efficiency. To maintain chromatographic efficiency, unions with internal channel diameters as small as 10 μm were specially produced for connecting packed capillaries to replaceable nanoESI emitters having orifice diameters of 2−10 μm (depending on the packed capillary dimensions). Coupled on-line with a hybrid-quadrupole time-of-flight MS through the nanoESI interface, the nanoLC separations provided peak capacities of ∼10^3 for proteome proteolytic polypeptide mixtures when a positive feedback switching valve was used for quantitatively introducing samples. Over a relatively large range of sample loadings (e.g., 5−100 ng, and 50−500 ng of cellular proteolytic peptides for 14.9- and 29.7-μm-i.d. packed capillaries, respectively), the nanoLC/nanoESI MS response for low-abundance components of the complex mixtures was found to increase linearly with sample loading. The nanoLC/nanoESI-MS sensitivity also increased linearly with decreasing flow rate (or approximately inversely proportional to the square of the capillary inner diameter) in the flow range of 20−400 nL/min. Thus, except at the lower loadings, decreasing the separation capillary inner diameter has an effect equivalent to increasing sample loading, which is important for sample-limited proteomic applications. No significant effects on recovery of eluting polypeptides were observed using porous C18 particles with surface pores of 300-Å versus nonporous particles. Tandem MS analyses were also demonstrated using the high-efficiency nanoLC separations. Chromatographic elution time, MS response intensity, and mass measurement accuracy was examined between runs with a single column (with a single nanoESI emitter), between different columns (same and different inner diameters with different nanoESI emitters), and for different samples (various concentrations of cellular proteolytic peptides) and demonstrated robust and reproducible sensitive analyses for complex proteomic samples.

Liquid chromatography (LC) high-efficiency separations or low- to moderate-efficiency LC involving two-dimensional separations have been previously coupled on-line with mass spectrometry (MS or tandem MS) through using electrospray ionization (ESI) for characterizing complex mixtures such as proteomic samples.[1−8] Liquid-phase separations yielding chromatographic peak capacities (at unit resolution[9]) on the order of 10^3 can be referred to as high efficiency, 10^2 as moderate efficiency, and 10^1 as low efficiency. High-efficiency separations are generally desired for resolving extremely complex mixtures such as global cellular enzymatic digests, which can contain >10^5 different peptide components.[2] Separation efficiency (or total peak capacity) improvements have resulted in ∼3-fold increases in the number of detected polypeptides using ESI Fourier transform ion cyclotron resonance (FTICR) MS for proteomic analyses[1] and ∼40% increase using ESI ion-trap MS/MS[8] due to factors that include better use of the MS dynamic range and reduced discrimination during ionization.

(1) Shen, Y.; Zhao, R.; Belov, M. E.; Conrads, T. P.; Anderson, G. A.; Tang, K.; Pasa-Tolic, L.; Veenstra, T. D.; Lipton, M. S.; Udseth, H.; Smith, R. D. *Anal. Chem*. **2001**, *73*, 1766−1775.
(2) Shen, Y.; Tolic, N.; Zhao, R.; Pasa-Tolic, L.; Li, L.; Berger, S. J.; Belov, M. E.; Smith, R. D. *Anal. Chem*. **2001**, *73*, 3001−3021.
(3) Li, L.; Masselon, C. D.; Anderson, G. A.; Pasa-Tolic, L.; Lee, S. W.; Shen. Y.; Zhao, R.; Lipton, M. S.; Conrads, T. P.; Tolic, N.; Udseth, H.; Smith, R. D. *Anal. Chem*. **2001**, *73*, 3312−3322.
(4) Link, A. J.; Eng, J.; Schieltz, D. M.; Carmack, E.; Mize, G. J.; Morris, D. R.; Garvik, B. M.; Yates, J. R. *Nat. Biotechnol*. **1999**, *17*, 676−682.
(5) Washburn, M. P.; Wolters, D.; Yates, J. R. *Nat. Biotechnol*. **2001**, *19*, 242−247.
(6) Wall, D. B.; Kachman, M. T.; Gong, S.; Hinderer, R.; Parus, S.; Misek, D. E.; Hanash, S. M.; Lubman, D. M. *Anal. Chem*. **2000**, *72*, 1099−1111.
(7) Timperman, A.; Aebersold, R. *Anal. Chem*. **2000**, *72*, 4115−4121.
(8) Davis, M. T.; Beierle, J.; Bures, E. T.; McGinley, M. D.; Mort, J.; Robinson, J. H.; Spahr, C. S.; Yu, W.; Luethy, R.; Patterson, S. D. *J. Chromatogr., B* **2001**, *752*, 281−291.
(9) Giddings, J. C. *United Separation Science*; John Wiley & Sons: New York, 1991; p 105.

10.1021/ac0202280 CCC: $22.00
Published on Web 07/03/2002

Additionally, narrower peaks achieved in high-efficiency separations also provide higher concentrations for low-abundance species, enabling more sensitive MS detection.

The reduction of sample sizes is of general interest in bioanalyses. For example, the heterogeneous nature of cells and tissues[10] can result in the need for analysis of limited subpopulations. Proteome analysis for such small amounts of protein mixtures presents challenges for both separation and detection sensitivity, especially considering the range of protein abundances.[11] In mammalian proteomics, often only limited cell numbers (e.g., 10^3-10^5 cells, corresponding to protein contents of ~0.1−10 μg) are available. Very small samples obtained using methods such as laser capture microdissection techniques[12] yield tissue volumes measured in cubic micrometers and sample sizes generally in the submicrogram range. Based on such limited sample quantities, attention to every step of sample processing (e.g., cell lysis, stable isotopic labeling, protein extraction, and enzymatic digestion) is necessary to optimize the sensitivity and dynamic range of detection.

Currently, ESI is the dominant technique for on-line LC/MS coupling.[13−16] Miniaturizing the separation column inner diameter improves ESI-MS sensitivity, which often "behaves as if it were a concentration sensitive detector".[14−16] The concentration of equally abundant solutes in the LC mobile phase is proportional to the inverse square of the column inner diameter (assuming that columns have the same porosity and provide the same efficiency), which substantially determines the ESI-MS signal. Banks demonstrated that LC/MS response increased 163-fold by decreasing the LC mobile-phase flow from 1000 to 1.8 μL/min by reducing the column diameter from 4.6 to 0.25 mm.[17] In the submicroflow (<1 μL/min) range, ESI-MS performances have been extensively investigated using direct infusion of a specific concentration sample or with capillary electrophoresis (CE).[18−22] Oosterkamp et al. reported that, up to 400 nL/min, the ESI (using an emitter orifice of 25 μm) MS responds linearly with direct infusion of a 0.2 pmol/μL analyte, i.e., a mass-dependent response in the low-flow range and mass-independent behavior at higher flow rate.[18] With a similar approach (emitter orifice of 20 μm), Bateman et al. also observed similar ESI-MS behavior in the flow range of <170 nL/min for direct infusion of a 10 μg/mL Leu-enkephalin.[19] With CE, it has been demonstrated that ESI-MS sensitivity increases by a factor of 25−50 upon reducing the CE column inner diameter from 100 to 5 μm (to estimated flow rates of a couple nanoliters per minute),[20−22] consistent with concentration-dependent behavior. (It should be noted that the "concentration" referred to in column separations is different from that of the original samples injected, but corresponds to the sample concentrations eluting from the separation column, which are determined by the sample mass injected, the column effective void volume, and the separation efficiency or peak width.) For a specific separation column, increasing sample loading results in an equivalent increase in its concentration, assuming the same separation quality or the sample zone length in the column remains constant. This situation is different from sample direct infusion, where the analyte mass quantity can be manipulated by changing the flow rate for a solution of a given analyte concentration. The "concentration-sensitive" behavior of LC/ESI-MS provides the basis for improving its sensitivity by using narrower diameter separation columns providing lower flow rates, while operation in the regime where the response to the mass quantity loaded on the column is linear is most attractive for quantitative analyses.

Packed capillary LC has been practiced for more than twenty years.[23−30] Although packed capillary LC with 150-μm-i.d. columns (5-μm packing particles) has been considered as nanoscale LC (or nanoLC, the flow at nanoliter per minute, or nanoflow),[31] we limit the designation to packed capillaries having inner diameters of <75 μm, where submicroliter per minute flow rates exist when these capillaries are packed with media of various porosities and operated at their optimal linear velocities. The chromatographic performance of ~50−75-μm-i.d. packed capillaries has previously been evaluated,[32,33] and such formats are increasingly used for LC/MS analyses.[4,18,34−38] Extension to smaller inner diameter (<50 μm) packed capillaries with flows of <100 nL/min will be important for optimization of sensitivity, and such packed capillaries have been introduced by Jorgenson and co-workers.[39,40] Capillaries of 21−50-μm i.d. with 30−35-cm lengths using 5-μm porous particles were prepared by slurry packing and the chro-

(10) Heppner, G. H.; Miller, F. R. *Int. Rev. Cytol.* **1998**, *177*, 1−56.
(11) Corthals, G. L.; Wasinger, V. C.; Hochstrasser, D. F.; Sanchez, J.-C. *Electrophoresis* **2000**, *21*, 1104−1115.
(12) Bonner, R. F.; Emmert-Buck, M. R.; Cole, K.; Pohida, T.; Chuaqui, R.; Goldstein, S.; Liotta, L. A. *Science* **1997**, *278*, 1481−1483.
(13) Abian, J.; Oosterkamp, A. J.; Gelpí, E. *J. Mass Spectrom.* **1999**, *34*, 244−254.
(14) Bruins, A. P.; Covey, T. R.; Henion, J. D. *Anal. Chem.* **1987**, *59*, 2642−2644.
(15) Bruins, A. P. *Mass Spectrom. Rev.* **1991**, *10*, 53−77.
(16) Hopfgartner, G.; Bean, K.; Henion, J. *J. Chromatogr.* **1993**, *647*, 51−61.
(17) Banks, J. F., Jr. *J. Chromatogr.* **1996**, *743*, 99−104.
(18) Oosterkamp, A. J.; Gelpí, E.; Abian, J. *J. Mass Spectrom.* **1998**, *33*, 976−983.
(19) Bateman, K. P.; White, R. L.; Thibault, P. *Rapid Commun. Mass Spectrom.* **1997**, *11*, 307−315.
(20) Goodlet, D. R.; Wahl, J. H.; Udseth, H. R.; Smith, R. D. *J. Microcolumn Sep.* **1993**, *5*, 57−62.
(21) Wahl, J. H.; Goodlett, D. R.; Udseth, H. R.; Smith, R. D. *Electrophoresis* **1993**, *14*, 448−457.
(22) Smith, R. D.; Wahl, J. H.; Goodlett, D. R.; Hofstadler, S. A. *Anal. Chem.* **1993**, *65*, 574A−584A.
(23) Novotny, M., Ishii, D., Eds. *Microcolumn Separations*; Elsevier: Amsterdam, 1985.
(24) Ishii, D.; Asai, K.; Hibi, K.; Jonokuchi, T.; Nagaya, M. *J. Chromatogr.* **1977**, *144*, 157−168.
(25) Yang, F. J. *J. Chromatogr.* **1982**, *236*, 265−277.
(26) Takeuchi, T.; Ishii, D. *J. Chromatogr.* **1982**, *238*, 409−418.
(27) Gluckman, J. C.; Hirose, A.; McGuffin, V. L.; Novotney, M. *Chromatographia* **1983**, *17*, 303−309.
(28) Novotny, M.; Hirose, A.; Wiesler, D. *Anal. Chem.* **1984**, *56*,1243−1248.
(29) Borra, C.; Soon, M. H.; Novotny, M. *J. Chromatogr.* **1987**, *365*, 75−85.
(30) Hoffmann, S.; Blomberg, L. *Chromatographia* **1987**, *24*, 416−420.
(31) Chervet, J. P.; Ursem, M.; Salzmann, J. P. *Anal. Chem.* **1996**, *68*, 1507−1512.
(32) Karlsson, K-.E.; Novotny, M. *Anal. Chem.* **1988**, *60*, 1662−1665.
(33) Cole, L. J.; Schultz, N. M.; Kennedy, R. T. *J. Microcolumn Sep.* **1993**, *5*, 433−439.
(34) Hose, I.; Van Dongen, W.; Lemière, F.; Esmans, E. L.; Van Bockstaele, D.; Berneman, Z. N. *J. Chromatogr., B* **2000**, *748*, 197−212.
(35) Martin, S. E.; Shabanowitz, J.; Hunt, D. F.; Marto, J. A. *Anal. Chem.* **2000**, *72*, 4266−4274.
(36) Quenzer, T. L.; Emmett, M. R.; Hendrickson, C. L.; Kelly, P. H.; Marshall, A. G. *Anal. Chem.* **2001**, *73*, 1721−1725.
(37) Vanhoutte, K.; Van Dongen, W.; Hoes, I.; Lemière, Esmans, E. L.; Van Onckelen, H.; Van den Eeckhout, E.; van Soest, R. E. J.; Hudson, A. J. *Anal. Chem.* **1997**, *69*, 3161−3168.
(38) Vanhoutte, K.; Van Dongen, W.; Esmans, E. L. *Rapid Commun. Mass Spectrom.* **1998**, *12*, 15−24.
(39) Kennedy, R. T.; Jorgensen, J. W. *Anal. Chem.* **1989**, *61*, 1128−1135.
(40) Hsieh, S.; Jorgenson, J. W. *Anal. Chem.* **1996**, *68*, 1212−1217.

matographic (mainly, kinetic) performance was evaluated.[39] For inner diameters of 12−33 μm, they found that a high column efficiency (e.g., reduced plate height of ∼1.0) could be achieved with a small ratio of column inner diameter to particle size (e.g., ∼2.2 for their 12-μm-i.d. capillary containing particles with average size of 5.44 μm).[40] However, no column length or total separation efficiencies were reported for these 12−33-μm-i.d. packed capillaries (the column lengths are generally limited by the packing pressure). Recently, the same group described an ultrahigh-pressure LC system,[41] where an efficient separation (peak capacity of ∼300 in ∼30 min) for an ovalbumin tryptic digest was demonstrated.[42] In this separation, a 27 cm × 30 μm i.d. capillary packed with 1.0-μm C18-bonded nonporous particles was investigated in a chromatographic system utilizing very high pressure (37 kpsi) solvent delivery and laser-induced fluorescence detection. A similar approach has also been investigated by Lee and co-workers for fast nanoLC isocratic elution using relatively short columns.[43] When these packed narrow (e.g., 29-μm i.d.) capillaries were coupled to time-of-flight MS, however, significant peak broadening was observed due to the use of a sheath liquid interface. Efficiently coupling packed narrow capillaries (i.e., i.d. <50 μm) to MS through an ESI source still remains a challenge for high-efficiency LC/MS.

Coaxial sheath liquid ESI interfaces have been successfully used for small-flow CE (e.g., using 5-μm-i.d. capillaries) coupled with mass spectrometry.[20−22,44] The advantage of this interface is its flexibility for manipulation of the eluent properties to optimize ESI efficiency. However, the use of sheath liquid can reduce sensitivity due primarily to the introduction of additional charge-carrying species from the sheath liquid. A sheathless MS interface was used by Smith and co-workers in their first work with coupling CE,[45,46] and an improved contoured sheathless CE/MS interface was first demonstrated in 1993.[22] Wilm and Mann used a sheathless nanoelectrospray ionization (nanoESI) source using a gold-coated pulled glass capillary emitter with an orifice of 1−2-μm i.d. to allow flow rates as small as ∼20 nL/min.[47] The small orifice increased the stability of the electrospray, resulting in a more uniform smaller average droplet size and an improvement in ESI-MS performance.[48] However, an ESI emitter orifice of 1−2 μm i.d imposes an additional pressure drop when used with nanoLC mobile-phase flows of >70 nL/min. Vanhoutte et al. used a 9-μm-i.d. orifice with 75-μm-i.d. packed capillary nanoLC.[38] Construction of an interface for nanoLC/nanoESI MS is complicated by the need to minimize postcolumn band broadening. Constructing an effective nanoESI emitter directly on the fused-silica capillary outlet (i.e., integrated packed capillary column) has the inherent advantage of minimizing the extra dead volume,[35] but emitter failure also destroys the column, an obstacle to wide acceptance and routine application. Alternatively, connecting a preprepared, replaceable emitter to a prepacked capillary provides a convenient and flexible approach but may degrade separation quality due to the additional connection dead volume.

In this study, we have developed high-efficiency (peak capacities of $\sim 10^3$) nanoLC/nanoESI-MS for capillaries having dimensions of 87 cm × 15−75 μm i.d. packed with 3-μm particles and demonstrated their application for complex proteomic mixtures. The nanoLC/nanoESI MS dependence on sample-loading and mobile-phase flow rates in the low-nanoliter per minute range was examined using these packed capillaries. The implementation described was largely assembled using commercially available LC pumps and accessories, except for the ESI emitter connection union. The approach is shown to provide a robust and standardizable high-efficiency nanoLC/ESI MS system that can be readily adopted for a wide variety of bioanalytical applications, where routine analysis requires ultrahigh sensitivity or samples available in only limited quantity. Additionally, we show that this development provides the basis for improved absolute quantitation and the highest achievable LC/MS sensitivity.

EXPERIMENTAL SECTION

Packing of Long, Narrow Capillaries with 3-μm Particles. C18-bonded 3-μm porous (300-Å pores, Phenomenex, Torrance, CA) and nonporous particles (Micra Scientific, Northbrook, IL) were used as packing materials. The particle size distributions were examined using field emission scanning electron microscopy (SEM, LEO 982, D-73446, Oberkochen, Germany) with a measurement accuracy of 0.01 μm. For the porous particles, the average particle size was 3.6 μm with an average standard deviation of 14% (the particle sizes ranging from 5.7 to 1.9 μm) determined for 95 particles (Figure 1A). The choice of these particles was dictated by the commercial availability of high-quality silica matrix for 3-μm particles with large pore size (i.e., 300 Å) suitable for proteomic samples which challenge the stationary-phase properties due to the sample-wide range of ionic properties (e.g., acid/base) and size distributions (e.g., smaller digested peptides to large undigested proteins). The nonporous particles used (Figure 1B) had an average diameter of 2.7 μm and a particle size deviation of 5% with the particle range of 2.0−3.4 μm (determined for 107 particles).

Various inner diameters of fused-silica capillary tubing (Polymicro Technologies, Phoenix, AZ) were also characterized using SEM (Table 1). Capillaries were cut into ∼1-m lengths for packing. PEEK tubing (380-μm i.d., Upchurch Scientific, Oak Harbor, WA) was used to position a steel screen (2-μm pores, Valco Instruments, Houston, TX) and seal the fused-silica capillary in a homemade narrow-bore union (internal diameters from 10 to 50 μm). The union internal channel size was matched with the inner diameter of packed capillary, as indicated in Table 2. The other end of the capillary was connected to a stainless steel vessel (∼1.5 mL), in which the packing particles and a magnetic stirrer bar were placed. A solvent mixture (90% acetonitrile aqueous solution, v/v, HPLC grade, Aldrich, Milwaukee, WI) was delivered by a Haskel pump (DSHF-302, Haskel, Burbank, CA) to supply the packing pressure. For packing 30−75-μm-i.d. capillaries, 90% acetonitrile solution was directly used as the slurry solvent. The particles were suspended in the slurry solvent with a magnetic stirrer and then slowly delivered into the capillary by gradually

(41) MacNair, J. E.; Lewis, K. C.; Jorgenson, *Anal. Chem.* **1997**, *69*, 983−989.
(42) MacNair, J. E.; Patel, K. D.; Jorgenson, *Anal. Chem.* **1999**, *71*, 700−708.
(43) Lippert, J. A.; Xin. B.; Wu, N.; Lee, M. L. *J. Microcolumn Sep.* **1999**, *11*, 631−643.
(44) Wahl, J. H.; Goodlett, D. R.; Udseth, H. R.; Smith, R. D. *Anal. Chem.* **1992**, *64*, 3194−3196.
(45) Olivares, J. A.; Nguyen, N. T.; Yonker, C. R.; Smith, R. D. *Anal. Chem.* **1987**, *59*, 1230−1232.
(46) Smith, R. D.; Olivares, J. A.; Nguyen, N. T.; Udseth, H. R. *Anal. Chem.* **1988**, *60*, 436−441.
(47) Wilm, M.; Mann, M. *Anal. Chem.* **1996**, *68*, 1−8.
(48) Wilm, M.; Mann, M. *Int. J. Mass Spectrom. Ion Processes* **1994**, *136*, 167−180.

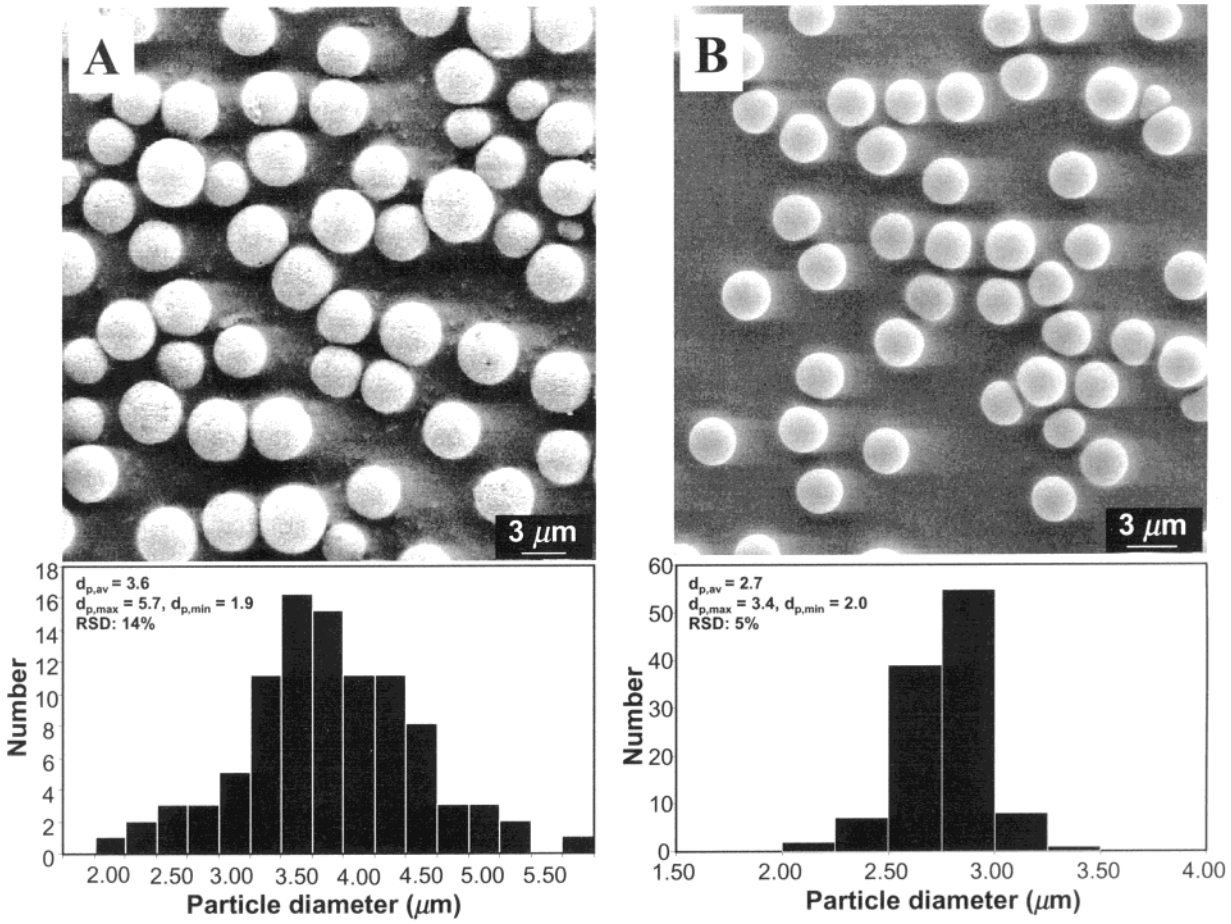

Figure 1. SEM analysis of (A) porous and (B) nonporous C18-bonded particles used for column production.

Table 1. NanoLC Packed Capillary Parameters Operated at 10 000 Psi[a]

columns (μm i.d. × cm)	d_p (μm)	p_d (Å)	u (cm/s)	F (nL/min)	γ	ϵ
porous						
74.5 × 87.0	3.6	300	0.19	393	20.7	0.78
47.1 × 87.0	3.6	300	0.19	155	13.1	0.79
29.7 × 87.0	3.6	300	0.22	76	8.3	0.81
19.8 × 87.0	3.6	300	0.22	33	5.5	0.81
14.9 × 87.0	3.6	300	0.23	20	4.1	0.83
nonporous						
29.7 × 87.0	2.8	∞	0.16	32	10.6	0.47
19.8 × 87.0	2.8	∞	0.17	15	7.1	0.49

[a] The capillary inner diameter (d_c) and particle size (d_p) were measured using SEM; linear velocity (u) and volume flow rate (F) were measured as described in the Experimental Section; p_d is the manufacturer specified pore size; γ is the ratio of column inner diameter to particle diameter; column porosity (ϵ) was calculated according to $\epsilon = 4F/\pi u d_c^2$.

Table 2. NanoESI Emitter Dimensions for High-Efficiency NanoLC[a]

column i.d (μm)	d_{union} (μm)	$d_{c,emit}$ (μm)	d_o t(μm)
74.5 (75)	50 ± 0.5	29.5 (30)	∼10
47.1 (50)	30 ± 0.5	19.8 (20)	∼7
29.7 (30)	20 ± 0.5	14.4 (15)	∼5
19.8 (20)	10 ± 0.5	11.7 (10)	∼3
14.9 (15)	10 ± 0.5	4.1 (6)	∼2

[a] d_{union} is the union internal channel diameter; $d_{c,emit}$ and d_o are the emitter capillary inner diameter and tapered orifice inner diameter, respectively; the values were measured with SEM and the values in parentheses are the manufacturer's specification.

increasing the pressure from 1000 to 18 000 psi. After filling ∼90 cm of the capillary, packing was stopped and the column was conditioned at 18 000 psi for ∼10 min in an ultrasonic bath and then left overnight to depressurize with a split flow of ∼15 μL/min. The packed capillary was cut to 87-cm length before use.

When using the acetonitrile aqueous solution (90%, v/v) to pack the smallest 14.9- and 19.8-μm-i.d. capillaries, we consistently observed particle aggregation after packing 30−60 cm. Immersing the column in an ultrasonic bath and pressurizing the column to 30 000 psi was insufficient to prevent aggregation. We evaluated various polarities and densities of solvents including hexane, dichloromethane, chloroform, tetrahydrofuran, methyl alcohol (and its aqueous solution), ethyl alcohol (and its aqueous solution), 2-propanol (and its aqueous solution), Triton-containing acetonitrile aqueous solution, and various mixtures of these solvents for producing a slurry−solvent suspension in the vessel. Successful packing was reproducibly obtained only with 2-propanol aqueous solutions. This solvent mixture is now being studied for packing of even smaller inner diameter (e.g., ∼10 μm) capillaries. Otherwise, procedures for packing these capillaries were identical to that for 30−75-μm-i.d. capillaries except for occasionally tapping the stainless steel vessel used for introducing the particles into the capillary. The column was first washed with 90% acetonitrile

aqueous solutions and then mobile phase A used in the LC separation.

Chromatographic parameters of these packed narrow capillaries were measured at a pressure of 10 000 psi and are given in Table 1. Linear velocities, which are of concern for optimizing overall separation efficiency, were measured using UV signal fluctuation from the injection as the marker for mobile phase A (H_2O with 0.2% acetic acid and 0.05% trifluoroacetic acid, TFA). The relatively fast liquid evaporation prevented accurately measuring the mobile-phase (volume) flow for these nanoscale columns using micropipettes (typically used for packed capillary LC flow rates of >1 μL/min). Instead, we measured the flow rate by placing two-UV detectors across a 14.7 cm × 47.1 μm i.d. open tubular capillary connected to the column outlet. The flow rate was calculated from the elution time of a marker through the two UV detectors. These accurately measured flow rates are necessary for calculating the column porosity and evaluating nanoESI-MS flow response. The capillary column porosity (ϵ) was determined using accurately measured capillary inner diameter, the mobile-phase linear velocity, and volume flow rates. As expected, ϵ increases with decrease in the ratio of capillary column inner diameter to particle size due to the increased capillary wall effect; the nonporous particle packed capillaries have much lower porosity than those containing porous particles. The difference in column porosity suggests that the useful estimates of some chromatographic properties should consider the effects of column porosity.

Preparation and Assembly of NanoESI Tip. NanoESI emitter tips were fabricated from 150-μm-o.d. fused-silica capillaries with inner diameters matching that of packed capillaries (see Table 2). Typically, the emitter capillary inner diameter was 30−50% of the packed capillary. The tip was drawn and tapered using a butane minitorch (Alltech, Deerfield, IL) when the capillary was flushed with liquid carbon dioxide (~600 psi) at room temperature, allowing controlled generation of tips having very thin walls. Further cutting adjusted the orifice size for various mobile-phase flows of different dimensions of packed capillaries (see Table 2; the emitter orifice inner diameters varied slightly). These thin-wall emitter tips provided a higher sensitivity than the equivalent diameter orifice having a thick wall made by tapering and then cutting without use of the high-pressure carbon dioxide.

The tapered nanoESI emitter was connected to the packed capillary column using a union and PEEK tubing, as illustrated in Figure 2 (bottom). The union body was purchased from Valco and was modified to contain internal channels having diameters from 10 to 50 μm with alignment and size variances of ±0.5 μm. The union internal channel diameter (d_{union}) depended on the inner diameter of the separation packed capillaries (d_c), and typically, the d_{union} selected was between 0.5 and 1 times of d_c. Too small a union internal diameter degraded separation efficiency due to the large unswept dead volume. The PEEK tubing inner diameter should be as close as possible to the outer diameter of the fused-silica capillary and was critical for achieving high-efficiency nanoLC/nanoESI MS; thus, 150-μm-i.d. PEEK tubing was used to connect the emitter (~150-μm-o.d. fused-silica capillary). Table 2 lists the union internal diameters used for various packed capillaries. The total volume of the union and the emitter is <1.5% of the packed capillary void volume.

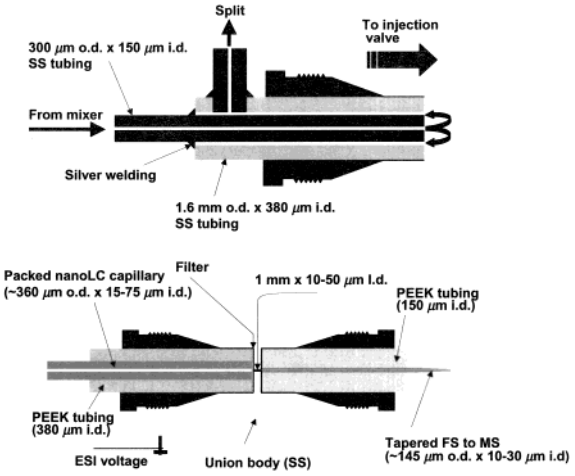

Figure 2. Assembly diagrams of gradient splitter (upper) and narrow packed capillary/nanoESI tubing connection module (bottom).

NanoLC Experiments. The NanoLC studies were carried out as described previously using sample introduction with a positive-feedback six-port switching valve.[2] The sample loop (200 nL) was made from 11.5 cm × 47.1 μm i.d. fused-silica capillary, and separations were carried out under constant pressure (10 000 psi) with the exponential gradient; the gradient curve can be seen in refs 1 and 2. To minimize delay for the mobile-phase gradient, an improvement in mobile-phase delivery prior to the injection valve was implemented by an arrangement of "tubing in tubing" as illustrated in Figure 2. The mobile-phase split (~12.5 μL/min) thus occurs just before the switching valve port, which minimizes the extra volume prior to the separation packed capillary. The void volume of the injector is estimated as ~40 nL from two adapter ports (dimension: 1 mm × 150 μm i.d.) of the valve, and the channel volume is negligible (the rotor was checked by microscopy and the channel becomes very small after use at 10 000 psi). This reduced void volume resulted in <2-min gradient delay, even for the 14.9-μm-i.d. packed capillary (flow rate of ~20 nL/min; see Table 1) if the injector is switched back to the injection position after sample loading. This delay is negligible for our high-efficiency separations lasting ~3 h.

MS and Tandem MS (MS/MS) Experiments. A hybrid-quadrupole time-of-light (Q-TOF) mass spectrometer (API QSTAR Pulsar, PE-Sciex, Toronto, Canada) was used to examine nanoLC/nanoESI-MS performance. The heated capillary and electrospray voltage were operated in ranges of 100−130 °C and 1.2−1.6 kV, respectively, depending on the mobile-phase flow. The mass spectrometer was fitted with an ion funnel interface,[49] which was operated at 500 kHz, a dc electric field of 2.00−2.65 V/mm, and rf amplitude of 45−50 V peak to peak. The Q-TOF was operated with the QS version of Analyst software. The pressure in the ion funnel region was 1.4 Torr. The emitter orifice was positioned at ~3 mm from the heated capillary ion inlet. The total MS acquisition cycle of 2.5 s was used for MS experiments and 5.0 s for data-dependent MS/MS experiments. Data-dependent MS/MS consisted of one initial MS scan of 2 s followed by one MS/MS scan of 3 s. The window of dynamic exclusion time was 6 s, and only peptides with m/z over 400 and intensities greater than 10 counts/s were selected for MS/MS.

(49) Shaffer S. A.; Anderson G. A.; Udseth H. R.; Smith R. D. *Anal. Chem.* **1998**, *70*, 4111−4119.

Cellular Protein Extract Tryptic Digest. A global soluble yeast protein proteolytic digest was used to test the performance of nanoLC/nanoESI MS. A procedure similar to that previously reported[2] was used to generate this sample. Haploid yeast BY4702 (ATCC No. 200867) was grown at 30 °C in YPD broth to mid-log phase ($OD_{600} = 6.0$). A cell pellet was obtained by centrifugation (3000*g*, 15 min, 4 °C) and was washed once with cold distilled water. The washed pellet was resuspended in three volumes of lysis buffer (50 mM Tris-acetate at pH 7.0, 50 mM NH_4Cl, 12 mM $MgCl_2$), and cells were disrupted by three cycles of French press (16 000 psi). The lysate was centrifuged twice (JA-20 rotor, 30000*g*, 30 and 20 min, 4 °C) to remove cell debris, and the spun lysate was quick-frozen with liquid nitrogen and stored at −80 °C. Cytosol (22 mg/mL) was produced by ultracentrifugation (100000*g* at 4 °C for 15 min). Yeast cytosol (5 mg/mL) in 1.0 M urea, 50 mM Tris (pH 8.0 at room temperature), 2 mM $CaCl_2$ was heated to 90 °C for 3 min and then cooled to ambient temperature. Trypsin (1:100, w/w, Promega Modified Sequencing Grade, Madison, WI) was added, and the mixture was incubated at 37 °C overnight. Following centrifugation (17000*g*, 15 min, 4 °C) of insoluble material, additional trypsin (1:40, w/w) was added, and the mixture was incubated for an additional day. Aliquots were quick-frozen and stored at −80 °C until analyzed.

RESULTS AND DISCUSSION

High-Efficiency NanoLC/NanoESI MS. Complex mixtures are generally separated by LC using mobile-phase gradients, and the determination of peak capacity[9] for applications to complex mixtures is the most practical way to evaluate LC separation quality and power. An attraction of MS detection is the ability to characterize chromatographically coeluted components (generally unavoidable for complex mixtures). Figure 3 shows nanoLC/nanoESI-MS for 100 ng of a yeast soluble protein tryptic digest obtained using an 87 cm × 19.8 μm i.d. capillary packed with 3-μm C18-bonded porous (300-Å pores) particles. The mobile phase flow is ~30 nL/min at the operating pressure of 10 000 psi. Peak elution began after ~20 min of gradient start and was completed in ~180 min. Symmetric peaks were observed through the entire separation. Peak broadening with increasing elution time[42] was not observed in this study due to high organic content (90%, v/v) in the mobile phase B causing analytes to be eluted in less than 65% B, which is prior to the flatter portion of the exponential gradient curve.[1] The use of constant-pressure operation allows a flexible and convenient utilization of the mobile-phase flow for other operations, such as on-line sample trapping (to be reported elsewhere) and multiple-capillary separations using a single pumping system.[2] Operated at constant pressure with static mobile-phase mixing, the mobile-phase gradient is very smooth and reproducible (see discussion below). If necessary, the gradient speed can be manipulated by adjusting the split flow.

The separation quality was estimated by examining the elution profile of individual sample components on extracted ion chromatograms. Figure 4 demonstrates an elution profile for a moderate-intensity peak from the separation in Figure 3. During the overall separation time of 150 min (from 20 to 170 min; see Figure 3), the separation yields a peak capacity of ~1100 (peak capacity calculated as in ref 9). Across the entire elution window, 15 peaks with intensities of <300 counts/s were used to calculate the peak capacity using the same procedure as in Figure 4, and an average peak capacity of 1088 was obtained with the highest of 1260 and the lowest 936. This separation power can resolve four or five peaks in 1 min (see Figure 3). The separation quality achieved in this study of nanoLC is similar to that previously reported using 150-μm-i.d packed capillaries.[1] This suggests that high-efficiency (peak capacities of $\sim 10^3$) nanoLC can be achieved with MS through using nanoESI, if extracolumn void volumes are minimized. Careful attention to tubing connections for mobile-phase gradient split (Figure 2) permitted switching valve sample introduction to be successfully applied for gradient nanoLC with flow rates of <50 nL/min. The small internal diameter unions enable high-efficiency nanoLC/nanoESI-MS along with the easy replacement of ESI emitters. The separation quality for 14.9-, 29.7-, 47.1-, and 74.5-μm packed capillaries was also evaluated using the same approach, and very similar separation quality (peak capacities of $\sim 10^3$) was found.

Optimized Sample Loading for NanoLC/NanoESI-MS. Independent of the discussion of ESI-MS as a mass- or concentration-sensitive detector, increasing LC sample loading is often desirable (if sufficient sample is available) for MS detection because both mass and peak concentration are increased if separation quality is retained. For a complex sample having a wide range of relative abundances, low-abundance components can be better detected by increased sample loading. The maximum sample loading in LC/ESI-MS is limited by the column sample capacity (beyond which the separation quality degrades), as well as by possible effects due to the ESI process (discussed later). Our previous study has shown that an 85 cm × 150 μm i.d. packed capillary (containing 3-μm C18-bonded porous particles) is capable of loading up to hundreds of micrograms of polypeptides and that the number of detected peptide species increased from ~9000 to ~60 000 by increasing sample loading from 5 to 50 μg using FTICR.[1] Here, we further investigate nanoLC/nanoESI-MS response to sample loading for complex mixtures and the resultant sample capacity of combined nanoLC/nanoESI-MS.

Under identical experimental conditions, we loaded 25−1500 ng (by dilution to specific concentrations) of the sample onto a 29.7-μm-i.d. packed capillary. Figure 5 shows nanoLC/nanoESI-MS separations for sample loadings of 50, 100, 250, and 500 ng and demonstrates that many additional species become detectable with increased sample loading. To provide a conservative quantitative evaluation using the Q-TOF MS, only peaks with intensities of >40 counts/s (for which MS/MS is generally feasible) were counted. Increasing sample loading from 25 to 1000 ng raised the number of detected species from 144 to 2037, or ~14-fold. Using a 29.7-μm-i.d. packed capillary with a flow rate of ~75 nL/min, the Q-TOF MS detected only a limited number of peptides for <25 ng of this very complex polypeptide mixture. Studies using more sensitive mass spectrometers (e.g., FTICR)[50−52] should significantly decrease sample size requirements. However, any MS has its sensitivity limit, and the use of even smaller inner diameter packed capillaries may further improve the sensitivity for such complex mixtures.

(50) Marshall, A. G.; Hendrickson, C. L.; Jackson, G. S. *Mass Spectrom. Rev.* **1998**, *17*, 1−35.
(51) Paša-Tolić, L.; Jensen, P. K.; Anderson, G. A.; Lipton, M. S.; Peden, K. K.; Martinović, S.; Tolić, N.; Bruce, J. E.; Smith, R. D. *J. Am. Chem. Soc.* **1999**, *121*, 7949−7950.
(52) Belov, M. E.; Gorshkov, M. V.; Udseth, H. R.; Anderson, G. A.; Smith, R. D. *Anal. Chem.* **2000**, *72*, 2271−2279.

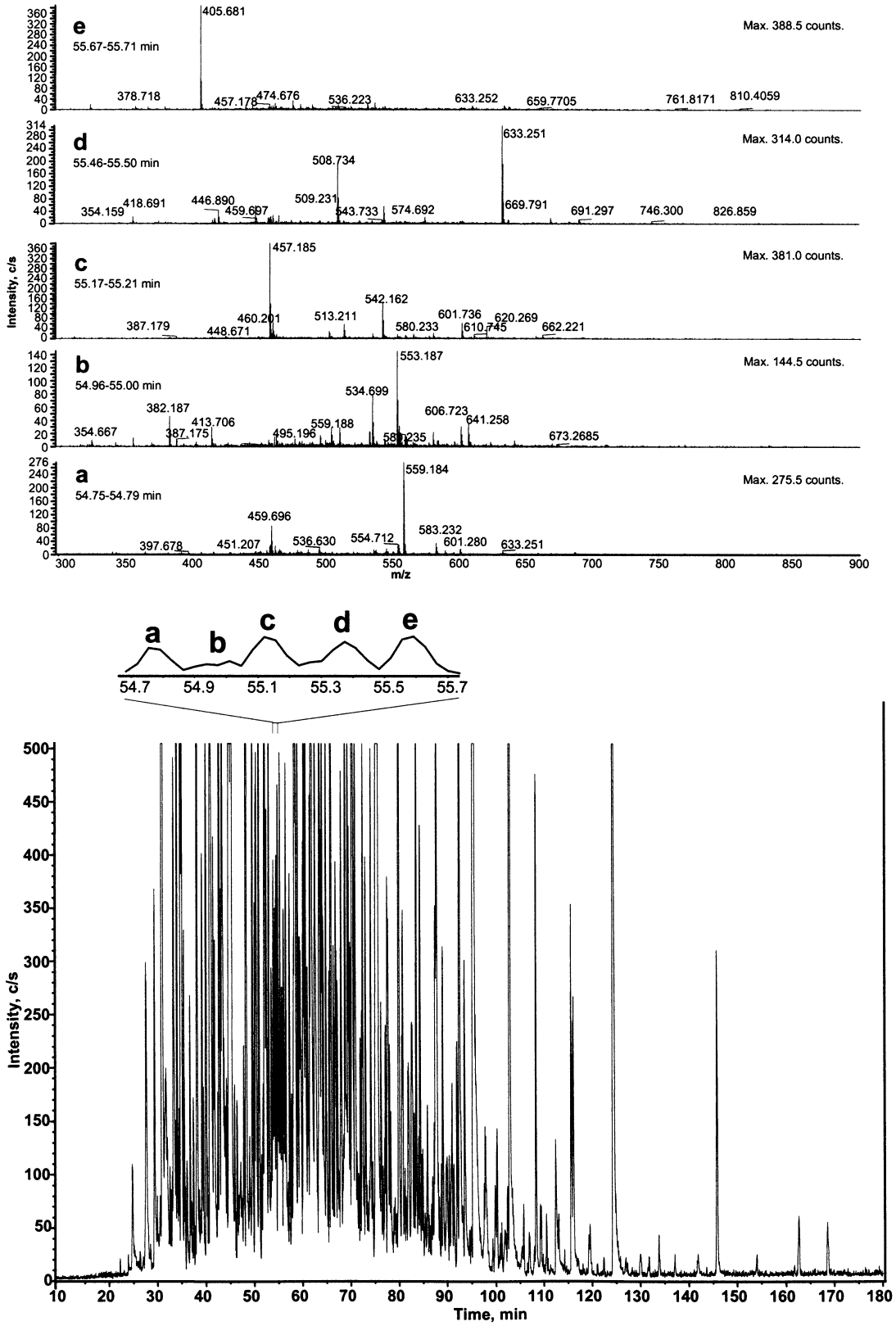

Figure 3. Base peak chromatogram and mass spectra for peaks in a 1-min window of the high-efficiency nanoLC/nanoESI-MS for 100 ng of a yeast soluble protein tryptic digest. Conditions: 87 cm × 19.8 μm i.d. fused-silica capillary packed with 3-μm porous C18-bonded particles (average particle size of 3.6 μm); 10 000 psi; mobile-phase gradient from A (H_2O, 0.2% acetic acid and 0.05% TFA) to 75% B (90% ACN, 10% H_2O, 0.1% TFA, v/v) in 200 min and data collection at the start of the gradient. A six-port positive-feedback switching valve with a sample loop of 200 nL was used for sample introduction.

The sample capacity or maximum sample loading was examined using a 29.7-μm-i.d. packed capillary column. Sample loadings of 1500 ng resulted in a peak broadening by ~30%, and we determined ~1000 ng as the maximum sample-loading amount

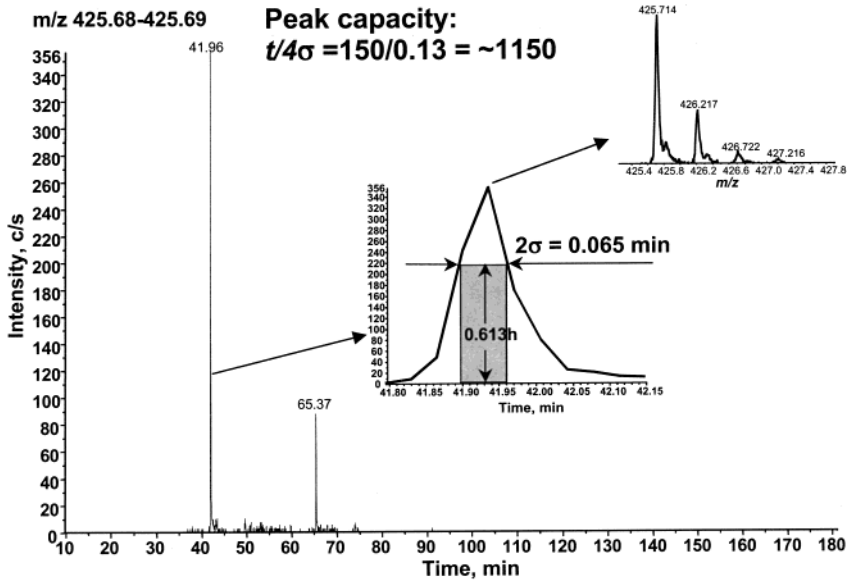

Figure 4. Peak capacity of the separation depicted in Figure 3 using extracted ion chromatograms and calculated according to ref 9.

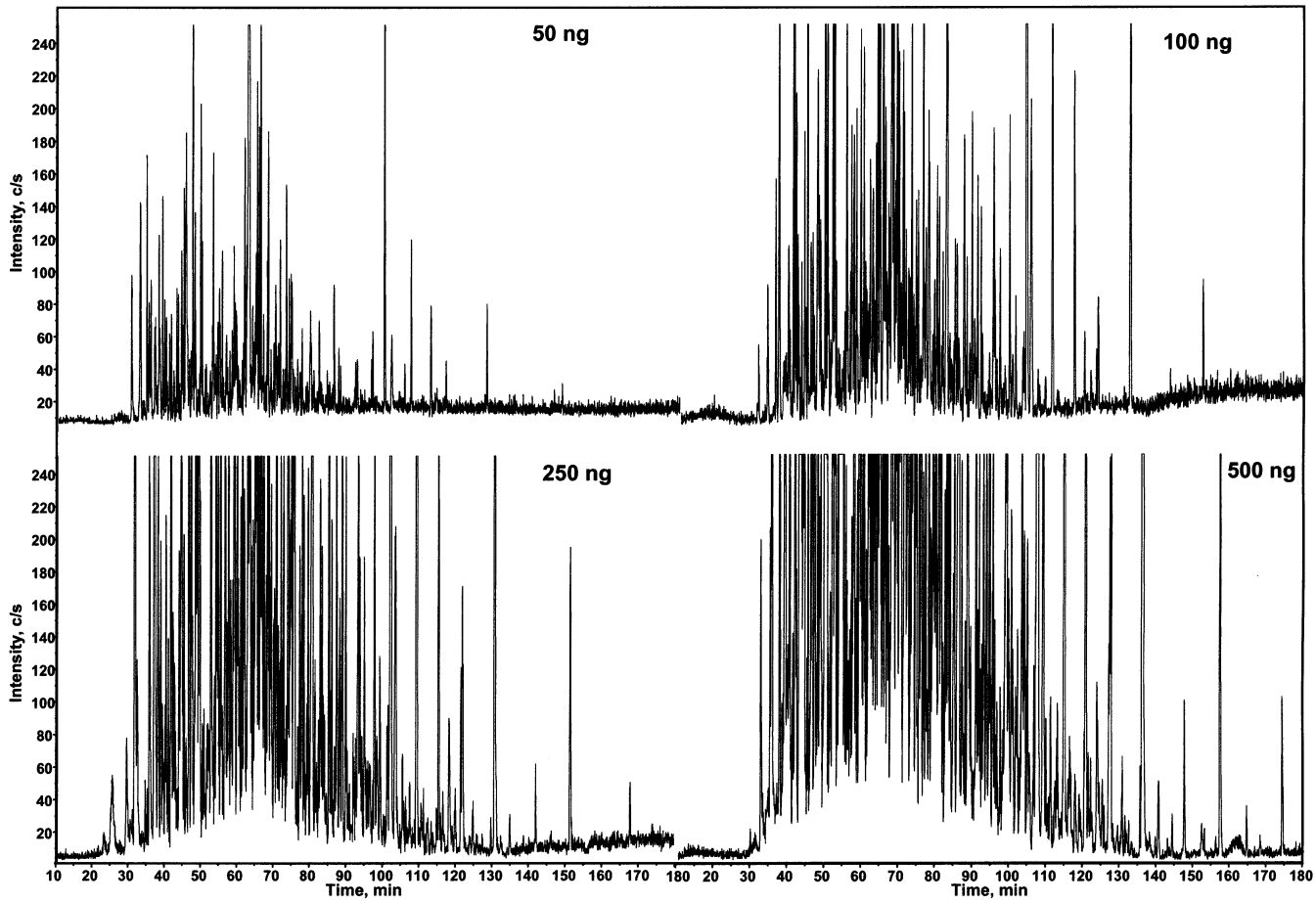

Figure 5. NanoLC/nanoESI-MS base peak chromatograms of a yeast soluble protein tryptic digest using various sample-loading amounts. Conditions: 87 cm × 29.7 μm i.d. fused-silica capillary packed with 3-μm porous C18-bonded particles. The sample loading amounts were labeled on the figures. Other conditions are the same as in Figure 3.

(i.e., sample capacity) of this column. The separation quality for loadings from 25 to 1000 ng was evaluated (data not shown) using the same procedure as in Figure 4, and equivalent separation efficiencies (peak capacities of $\sim 10^3$) were observed. Therefore, we simply used the intensity of MS peaks to characterize the relative ESI-MS response. Figure 6 shows the nanoESI-MS response for several components in the complex mixture with sample loadings of 25−1000 ng. The MS peak intensities of individual components in the complex mixture increased linearly with the total sample loading (and simultaneously, the total sample

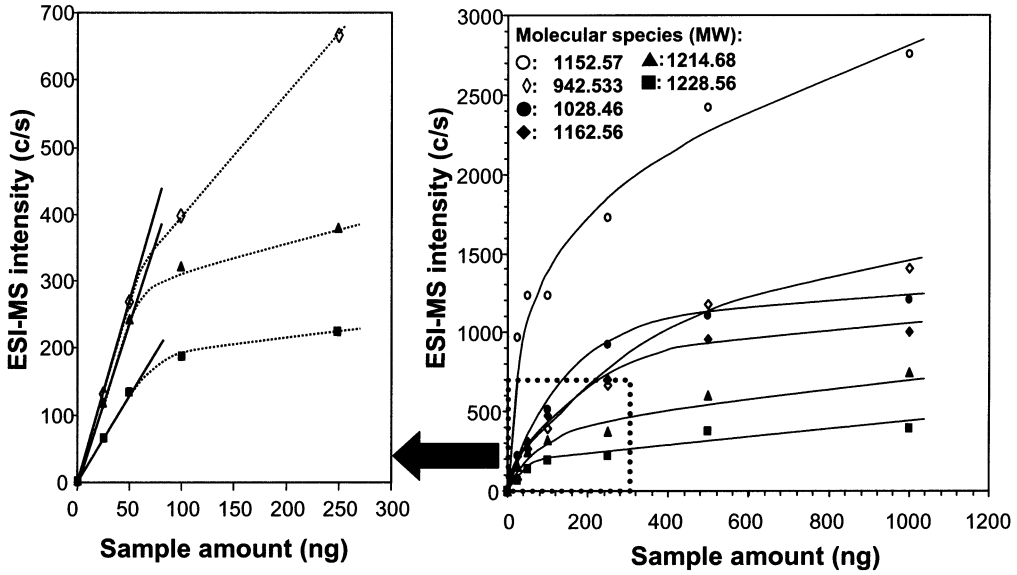

Figure 6. NanoLC/ESI-MS response of individual components in a global yeast tryptic digest to the total sample-loading amount. Conditions are the same as in Figure 5.

concentration in the column). Such "quantitative" behavior is observed for low sample loadings but "nonquantitative" behavior (i.e., nonlinear intermediate response, between "mass-sensitive" and "concentration-sensitive" behavior) is obtained for the higher loadings. This can be attributed to the ESI performance for higher peptide concentrations that effectively "compete" for the limited charge available on electrospray droplet surfaces (thus leading to increased "ion suppression" effect for some species).

The "nonquantitative" behavior of ESI, most evident for the use of small-diameter columns, has some significant implications for both quantitation and the dynamic range of measurements. Clearly, when dealing with complex mixtures having large differences in the relative concentrations of components, it is easily possible to encompass both mass- and concentration-limited detection behaviors in a single separation. Thus, the best quantitative results will be obtained for sample loadings that are sufficiently small so that the "quantitative" performance is obtained for all components (and where discrimination effects in ESI will also be minimal). However, such operation places the greatest demands upon ESI-MS sensitivity. On the other hand, the most reproducible performance (e.g., the best S/N) will be achieved with higher sample loadings, but where quantitation can be problematic for very complex samples where many components coelute and suppression effects will generally occur. These considerations lead us to point out an aspect of this behavior that can be advantageous. For complex samples, concentrations that span the range from "quantitative" to "nonquantitative" ESI performance at different elution times result in an effectively compressed dynamic range (ionization efficiency is suppressed for elution of more abundant components but is maximized for low abundance species). This can be of significant benefit in quantitative applications such as those involving MS/MS to identify peptides in complex mixtures. In such applications, the dynamic range of measurements will tend to extend beyond what would be expected based simply upon the relative abundances of sample component.

NanoLC/NanoESI-MS Sensitivity Dependence on Capillary Inner Diameter or Flow Rates (20−400 nL/min). Most studies of ESI-MS response have used direct infusion of a standard solution through an ESI emitter at different flow rates, a situation that differs from LC/ESI-MS, where a specific mass amount is introduced into the LC column and the concentration at the detector is a function of elution parameters. The measurement of LC/ESI-MS response to the flow is realized by use of different diameter columns (rather than a specific LC column with different flows, which can only be manipulated in a limited range by changing the mobile-phase linear velocity while maintaining optimal separation). Resolved analyte zones (peaks) elute to the ESI interface with a constant mass content, assuming various diameter columns generate the same separation efficiencies (or zone lengths). In this situation, the concentration of zones is proportional to the inverse of the flow, or approximately to the inverse square of the column inner diameter. The LC/ESI-MS response increase by decreasing the mobile-phase flows observed by Banks[17] can be more precisely attributed to the enhancement of ESI efficiency due to the greater concentration of analyte bands eluting from the smaller inner diameter columns.

Here, we explore the ESI-MS response to LC flow in a range of 20−400 nL/min by use of 14.9−74.5-μm-i.d. packed narrow capillaries and observe the expected dramatic changes in ESI-MS response. Figure 7 shows nanoLC/nanoESI-MS for 100 ng of a yeast soluble protein tryptic digest injected on to 74.5-, 47.1-, 29.7-, and 14.9-μm-i.d. packed capillaries (the corresponding flow rates for each capillary are given in Table 1). (It should be noted that the emitter orifice diameter used was also decreased (see Table 2) to account for the decrease in capillary column inner diameter and resultant flow changes.) Upon decreasing capillary inner diameter from 74.5 to 14.5 μm, the detected species (MS intensities of >40 counts/s) increased from 7 to 1345. We ascribe this gain to the increased concentration of components for peaks eluting the small inner diameter columns.

The nanoLC/nanoESI-MS response to the flow or capillary column inner diameter was further assessed using single ion extracted chromatograms from the complex mixture. Figure 8 shows the relationship between the nanoESI-MS response for 100

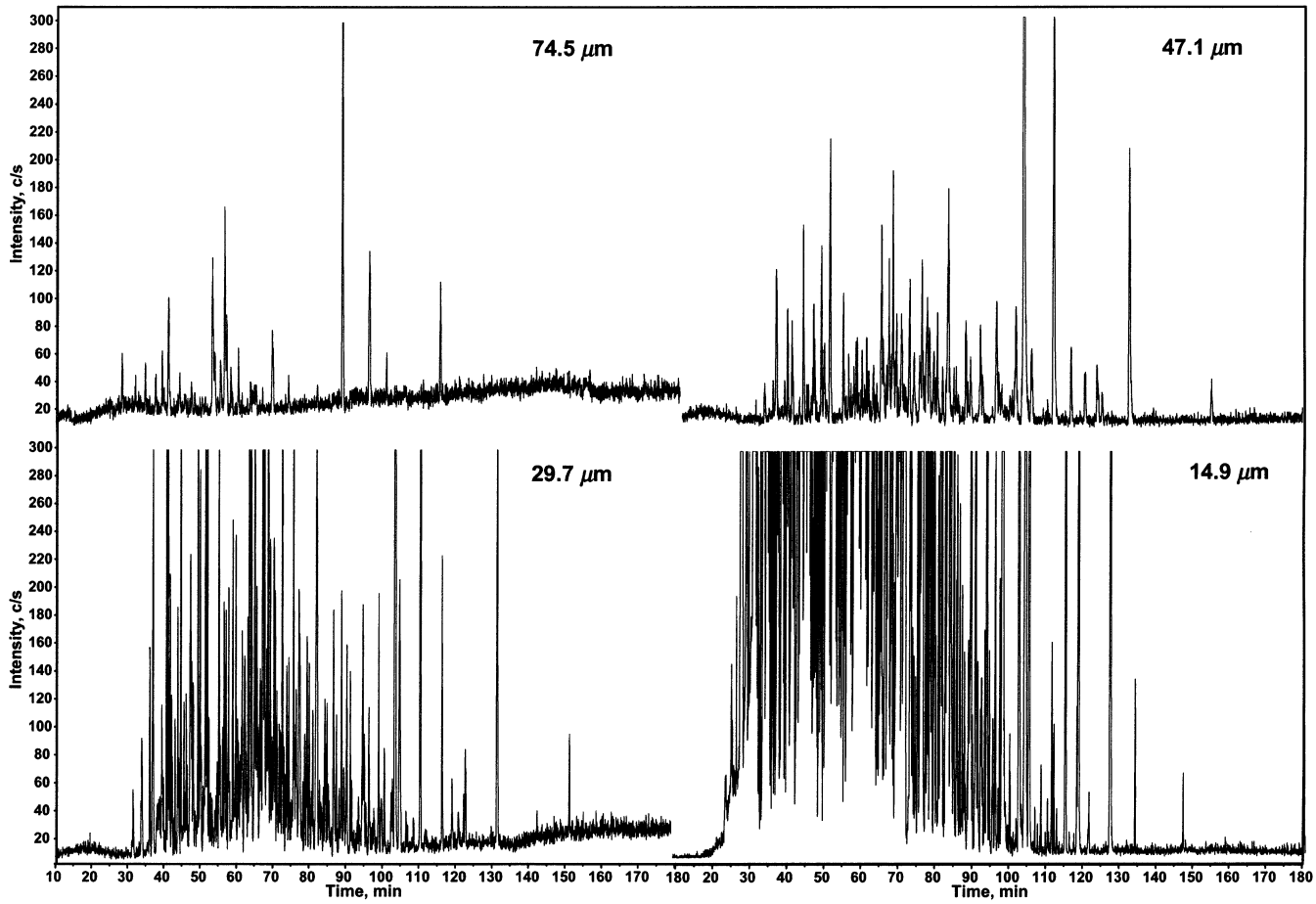

Figure 7. NanoLC/ESI-MS base peak chromatograms for 100 ng of a yeast soluble protein tryptic digest on 74.5-, 47.1-, 29.7-, and 14.9-μm-i.d. fused-silica packed capillaries. Conditions: all columns had a length of 87 cm, and the flow rates for various inner diameter columns were given in Table 1. Other conditions are the same as in Figure 3.

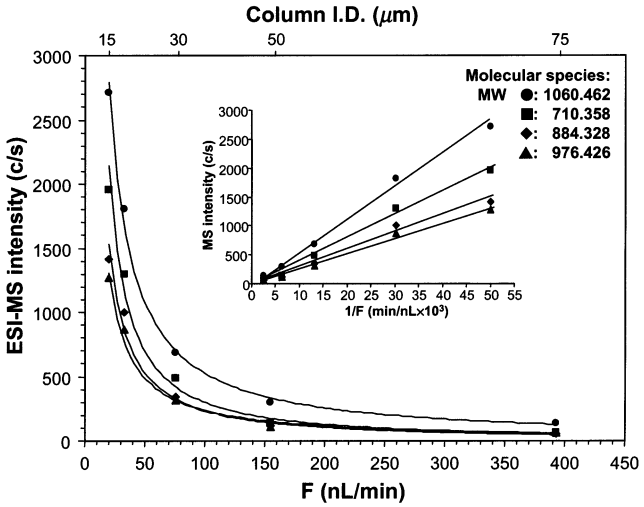

Figure 8. Relationship between nanoESI-MS response and the mobile-phase flow (or inner diameters) for individual species in the yeast soluble protein digest. Conditions: the flow rates were measured as described in the Experimental Section, and other conditions are the same as in Figure 7.

ng of the sample and mobile-phase flow/capillary column inner diameter. (The same separation quality, a peak capacity of $\sim 10^3$, was provided by these packed capillaries evaluated using the same procedure as in Figure 4.) The MS response shows a linear relationship between the nanoESI-MS response and the inverse of the mobile-phase flow in the range of 20−400 nL/min, which is a typical behavior of a "concentration-sensitive" detector. These results demonstrate the dramatic improvement in sensitivity by using small inner diameter columns. For proteome analyses, the narrowest packed capillaries that can provide sufficient sample capacity and robust operation will provide the best sensitivity for given sample loading.

Nonporous Packing Materials in NanoLC/NanoESI-MS. One of challenges associated with global proteome analyses is the large molecular weight distribution of the components. The sample interactions with the stationary phase in packed columns constitute one potential source influencing the sample recovery for various sample components. In our experiments with RPLC of proteome tryptic digests, C18-bonded reversed-phase particles (based on high-quality silica) with large surface pores (e.g., 300-Å pore size) were used to minimize the potential permanent retention of large polypeptides (and poorly digested proteins) within the surface pores. However, is a pore size of 300 Å large enough? Nonporous particles can be considered as having pores of infinite size, and their use will eliminate size-dependent analyte retention in pores. Furthermore, low mobile-phase flow rates of nonporous particle packed capillaries (due to their small column porosity; see Table 1) can indirectly benefit nanoESI efficiency. The disadvantages of nonporous particle packed capillaries include small solute retention and low sample capacity.

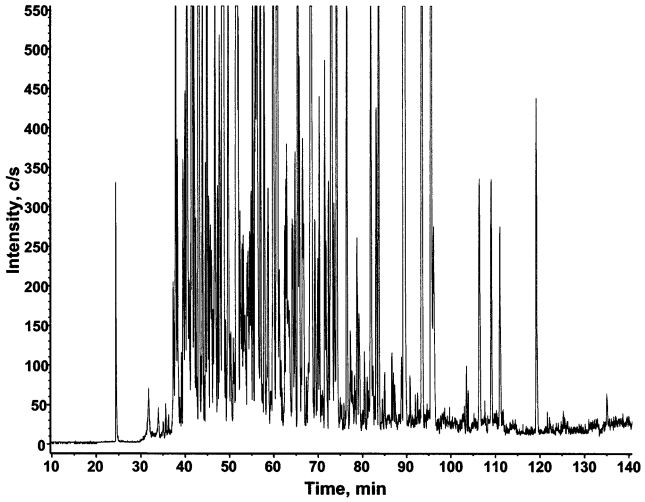

Figure 9. NanoLC/nanoESI-MS base peak chromatogram for 100 ng of a yeast soluble protein tryptic digest on an 87 cm × 29.7 μm i.d. fused-silica capillary packed with 3-μm nonporous C18-bonded particles (average particle size of 2.7 μm). Conditions were described in the text, and others are the same as in Figure 5.

Figure 9 shows nanoLC/nanoESI-MS for 100 ng of a yeast soluble tryptic digest obtained using a 3-μm C18-bonded nonporous particle packed 29.7-μm-i.d. capillary. The capillary was operated with a mobile-phase flow rate of 32 nL/min and was coupled to a ~3-μm-i.d. emitter orifice for nanoESI. Compared with the porous particle packed capillary column (Figure 5), the nonporous particle packed capillary speeds the separation (completed in ~140 min), consistent with the low specific area of the nonporous particle surface and resulting in lower retention. The peak capacity was ~650 over the separation window of 30−130 min. Approximately ~550 components were detected with intensities of >40 counts/s, similar to that achieved for a capillary packed with the porous particles and a flow rate of 76 nL/min. The fact that no significant gains in component detection were achieved using the nonporous particle packed capillary, even with the low flow rate, may be attributed to the lower resolving power of the nonporous packed capillary column and the accompanying high sample complexity delivered to the ESI interface.

The distributions of molecular sizes eluted from porous and nonporous particle packed capillaries were examined. No polypeptide size elution discrimination (up to 5000 Da) for the yeast tryptic digest was observed using the porous particle packed capillary versus nonporous particle packed capillary. This indicates that 300-Å pores should be sufficient for cellular global enzymatic digests. Currently, we prefer the use of porous particles for nanoLC/nanoESI-MS of complex proteomic samples because of the high resolving power and, simultaneously, a large sample capacity for packed narrow capillaries. However, the use of nonporous particles would be expected to provide higher sensitivity due to the lower flow rate, and the very small and uniform nonporous particles (e.g., ~1 μm) would make it possible to pack high-efficiency extremely small inner diameter capillaries (e.g., <10 μm). Equivalent quality, small diameter, large pore packing materials are difficult to synthesize and are generally unavailable.

NanoLC/NanoESI-MS/MS. Various types of mass spectrometers have been successfully used for tandem MS peptide identification including ion trap,[4,5,8,53−56] triple-quadrupole,[48,57−60]

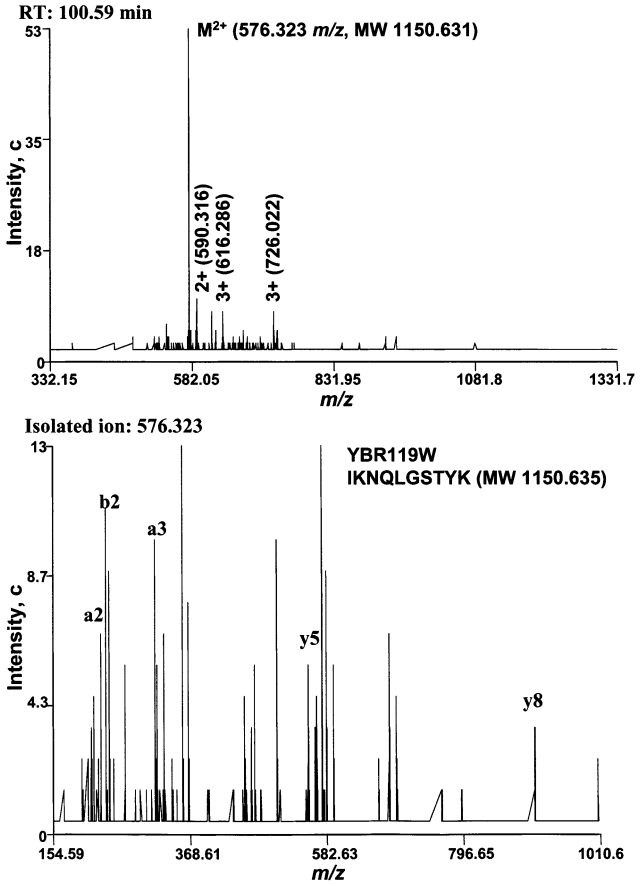

Figure 10. NanoLC/nanoESI-MS/MS for a low-intensity peptide (IKNQLGSTYK) from yeast protein YBR 119W. Conditions: chromatography conditions are the same as in Figure 5 except for loading 200 ng of the sample; data-dependent MS/MS conditions are described in the Experimental Section.

hybrid-quadrupole time-of-flight,[61−63] and FTICR[3,35,64−67] instruments. Tandem MS sensitivity depends on MS interface efficiency, ion selection efficiency, the subsequent ion fragmentation efficiency, and background noise levels, most of which are influenced by chromatographic conditions when an LC−ESI interface is used. While ESI-MS response under conditions where a stable electrospray is achieved will often correspond to only a fraction of flow rate for a given solution, LC/MS response will obviously be dependent upon all the attributes of a separation, and especially those that depend strongly on flow rate. Our previous studies[1,2]

(53) Timperman, A. T.; Aebersold, R. *Anal. Chem.* **2000**, *72*, 4114−4121.
(54) Yates, J. R., III.; Morgan, S. F.; Gatlin, C. L.; Griffin, P. R.; Eng, J. K. *Anal. Chem.* **1998**, *70*, 3557−3565.
(55) Marina, A.; Garcia, M. A.; Albar, J. P.; Yague, J.; Lopez de Castro, J. A.; Vazquez, J. *J. Mass Spectrom.* **1999**, *33*, 17−27.
(56) Gatlin, C. L.; Eng, J. K.; Cross, S. T.; Detter, J. C.; Yates, J. R., III. *Anal. Chem.* **2000**, *72*, 757−763.
(57) Cox, A. L.; Skipper, J.; Chen, Y.; Henderson R. A.; Darrow, T. L.; Shabanowitz, J.; Engelhard, V. H.; Hunt, D. F.; Slingluff, C. L., Jr. *Science* **1994**, *264*, 716−719.
(58) Wang, W.; Meadows, L. R.; den Haan, J. M.; Sherman, N. E.; Chen, Y.; Blokland, E.; Shabanowitz, J.; Agulnik, A. I.; Hendrickson, R. C.; Bishop, C. E. *Science* **1995**, *269*, 1588−1590.
(59) Shevchenko, A,; Wilm, M.; Vorm, O.; Mann, M. *Anal. Chem.* **1996**, *68*, 850−858.
(60) Figeys, D.; Ducret, A.; Yates, J. R., III; Aebersold, R. *Nat. Biotechnol.* **1996**, *14*, 1579−1583.
(61) Morris, H. R.; Paxton, T.; Panico, M.; McDowell, R.; Dell, A. *J. Protein Chem.* **1997**, *16*, 469−479.

Table 3. Reproducibility of Run to Run for High-Efficiency NanoLC/NanoESI-MS[a,b]

	m/z	RT (min)	I (c)	m/z	RT (min)	I (c)	m/z	RT (min)	I (c)	m/z	RT (min)	I (c)	m/z	RT (min)	I (c)
run 1	356.157	30.13	237	377.653	35.67	997	424.164	40.92	429	466.675	45.79	1600	475.678	50.46	617
run 2	356.159	30.79	351	377.657	36.08	916	424.168	41.33	572	466.675	46.12	1732	475.678	50.83	739
run 3	356.152	29.87	296	377.656	36.17	705	424.164	41.62	392	466.672	46.50	1816	475.674	51.17	640
av	356.156	30.26	294	377.656	35.97	873	424.165	41.29	464	466.674	46.14	1716	475.677	50.82	665
RSD	7.4×10^{-6}	1.1%	11%	3.5×10^{-6}	0.6%	13%	3.9×10^{-6}	0.6%	15%	2.9×10^{-6}	0.5%	5%	3.5×10^{-6}	0.5%	7%
run 1	505.225	56.04	371	513.243	61.17	414	488.214	66.38	683	552.219	71.13	454	463.715	76.08	796
run 2	505.228	56.50	497	513.246	61.75	655	488.218	66.96	970	552.226	71.50	650	463.715	76.46	1054
run 3	505.222	56.75	425	513.241	61.83	500	488.213	67.04	860	552.219	71.71	495	463.711	76.79	980
av	505.225	56.43	431	513.243	61.58	523	488.215	66.79	838	552.221	71.45	533	463.714	76.44	940
RSD	4.0×10^{-6}	0.5%	10%	3.9×10^{-6}	0.4%	17%	4.1×10^{-6}	0.4%	12%	5.4×10^{-6}	0.3%	22%	3.6×10^{-6}	0.3%	11%
run 1	509.714	80.79	696	465.717	85.25	298	949.389	91.00	90	576.244	96.26	2956	530.237	103.8	1577
run 2	509.719	81.00	687	465.718	85.37	429	949.396	90.88	116	576.245	96.25	3681	530.237	103.8	2159
run 3	509.714	81.45	567	465.712	85.92	318	949.389	91.41	95	576.241	97.17	3274	530.231	105.1	1825
av	509.716	81.08	650	465.716	85.51	348	949.391	91.10	100	576.243	96.56	3304	530.235	104.2	1854
RSD	4.6×10^{-6}	0.3%	5%	5.0×10^{-6}	0.3%	23%	3.2×10^{-6}	0.2%	10%	2.9×10^{-6}	0.3%	8%	5.0×10^{-6}	0.5%	11%
run 1	607.304	109.4	322	543.562	116.6	194	581.251	125.1	578	580.595	134.5	31	628.805	145.9	210
run 2	607.308	109.2	477	543.566	116.5	291	581.254	125.1	895	580.602	134.5	44	628.810	145.5	311
run 3	607.303	110.4	476	543.566	117.2	148	581.254	125.3	537	580.602	135.3	26	628.805	147.0	208
av	607.305	109.7	426	543.565	116.8	211	581.253	125.2	670	580.600	134.8	34	628.807	146.1	243
RSD	3.3×10^{-6}	0.3%	16%	3.1×10^{-6}	0.3%	25%	2.3×10^{-6}	0.1%	22%	5.2×10^{-6}	0.3%	21%	4.8×10^{-6}	0.4%	19%

[a] Conditions: an 87 cm × 19.8 μm i.d. capillary packed with 3-μm porous C18-bonded particles and equipped with a single ESI emitter (~3-μm-i.d. orifice) was used for three consecutive runs; 100 ng of a yeast soluble protein tryptic digest was used for each run; after each run, the column was conditioned with mobile phase A for 2.5 h; the peaks were randomly picked up across the elution time. Other chromatographic and MS detection conditions are the same as for Figure 3 and described in the Experimental Section. [b] $RSD_{m/z,\ total} = 4.1 \times 10^{-6}$; $RSD_{RT,\ total} = 0.4\%$; $RSD_{I,\ total} = 14\%$.

and the above discussion illustrate the importance of the chromatographic conditions for high-sensitivity LC/ESI-MS. Figure 10 demonstrates tandem MS of a low-intensity peptide peak (~50 counts/s) from a nanoLC/nanoESI-MS/MS of a yeast tryptic digest using a hybrid Q-TOF MS. The peptide was effectively fragmented to yield sufficient structural information for unique peptide identification (IKNQLGSTYK from yeast protein YBR119W). The mass calibration was performed before the MS/MS experiment (i.e., external), and the mass measurement accuracy for the parent peptide identification was ~3.5 ppm. The MS/MS capability of the hybrid Q-TOF MS used is expected to allow ~40-count MS peaks to be routinely identified using data-dependent nanoLC/nanoESI-MS/MS.

Reproducibility of NanoLC/NanoESI-MS. In this study, we investigated the nanoLC/nanoESI-MS (chromatographic elution and MS detection intensity and mass measurement) reproducibility based upon single ion extracted chromatograms using the yeast soluble protein tryptic digest as a model sample. The examined reproducibility includes run to run on a single column (with the same or different ESI emitters), column to column (having the same or different inner diameters with different ESI emitters in most situations), and sample to sample (with variances in sample concentration). Table 3 shows the run-to-run reproducibility for three successive nanoLC/nanoESI-MS runs using a 19.8-μm-i.d. packed capillary column with the same nanoESI emitter. Twenty ion chromatograms were extracted across the entire elution of the sample. With the hybrid Q-TOF MS used in this study, the experimental mass measurement accuracy was typically <8 ppm with an overall average of ~4 ppm for the 20 extracted species. The relative standard deviation (RSD) of chromatography elution time was ~0.5% for individual components (1.1% for the earliest eluting one) and the average RSD was 0.4% for the 20 species. This elution reproducibility level was comparable to that achieved using conventional LC. Using the same nanoESI emitter, the average RSD for nanoESI-MS intensities was 14% for the 20 extracted peaks (the largest variance was 25%). Reproducible nanoLC/nanoESI-MS enables one to better identify components of complex mixtures. Figure 11 shows two sets of mass spectra for two corresponding chromatographic peaks in two LC/MS runs. Almost exactly the same mass spectra (peaks and patterns) were found for corresponding chromatographic peaks. This is of critical importance for peptide identification using the accurate mass tag approach.[68,69] Other columns including 14.9- and 29.7-μm-i.d. packed capillaries were also examined, and a similar run-to-run reproducibility was observed.

Table 4 shows nanoLC/nanoESI-MS reproducibility of sample to sample for sample injections of 25−1000 ng using a 29.7-μm-i.d. packed capillary column with the same ESI emitter. The variance for mass measurement accuracy (average RSD of 6.4 ppm) was similar to that achieved for run-to-run experiments

(62) Kristensen, D. B.; Imamura, K.; Miyamoto, Y.; Yoshizato, K. *Electrophoresis* **2000**, *21*, 430−439.
(63) Graiffin, T. J.; Gygi, S. P.; Rist, B.; Aebersold, R.; Loboda, A.; Jilkine, A.; Ens, W.; Standing, K. G. *Anal. Chem.* **2001**, *73*, 978−986.
(64) Williams, E. R.; Loh, S. Y.; McLafferty, F. W.; Cody, R. B. *Anal. Chem.* **1990**, *62*, 698−703.
(65) Ross, C. W.; Guan, S. H.; Grosshans, P. B.; Ricca, T. L.; Marshall, A. G. *J. Am. Chem. Soc.* **1993**, *115*, 7854−7861.
(66) Masselon, C.; Anderson, G. A.; Harkewicz, R.; Bruce, J. E.; Paša-Tolić, L.; Smith, R. D. *Anal. Chem.* **2000**, *72*, 1918−1924.
(67) Håkansson, K.; Emmett, M. R.; Hendrickson, C. L.; Marshall, A. G. *Anal. Chem.* **2001**, *73*, 3605−3610.
(68) Conrads, T. P.; Anderson, G. A.; Veenstra, T. D.; Paša-Tolić, L.; Smith, R. D. *Anal. Chem.* **2000**, *72*, 3349−3354.
(69) Smith, R. D.; Anderson, G. A.; Paša-Tolić, L.; Lipton, M. S.; Shen, Y.; Conrads, T. P.; Veenstra, T. D.; Udseth, H. R. *Proteomics* **2002**, *2*, 513−523.

Table 4. Reproducibility of High-Efficiency NanoLC/NanoESI-MS for Loading Various Sample Amounts[a,b]

sample (ng)	*m/z*	RT (min)	*m/z*	RT (min)	*m/z*	RT (min)	*m/z*	RT (min)	*m/z*	RT (min)
25							554.792	34.67	488.257	40.92
50	560.721	38.42	541.225	42.67	462.217	58.21	554.790	67.50	488.257	70.37
100	560.725	41.08	541.229	45.04	462.220	60.33	554.792	69.33	488.257	73.29
250	560.717	39.96	541.219	44.46	462.214	60.42	554.785	69.50	488.249	73.62
500	560.717	42.29	541.220	47.50	462.218	63.08	554.789	71.69	488.252	76.25
1000	560.728	41.62	541.220	45.96	462.218	60.79	554.782	68.83	488.248	74.20
av	560.722	40.67	541.223	45.13	462.217	59.96	554.788	69.37	488.253	73.55
RSD	7.1×10^{-6}	3%	6.7×10^{-6}	3%	3.5×10^{-6}	2%	6.5×10^{-6}	1%	7.4×10^{-6}	2%
25	471.274	44.71	614.289	51.62	576.288	75.25	607.344	88.08	581.292	103.3
50	471.270	74.54	614.282	79.00	576.290	102.5	607.338	113.4	581.292	128.4
100	471.269	76.46	614.282	80.79	576.289	104.5	607.331	115.3	581.288	130.7
250	471.262	76.83	614.281	81.25	576.285	104.9	607.342	118.2	581.293	133.5
500	471.266	79.58	614.282	84.12	576.288	107.5	607.347	120.8	581.297	136.3
1000	471.258	77.42	614.272	82.25	576.278	106.0	607.342	119.5	581.285	134.9
av	471.265	76.97	614.280	81.48	576.286	105.5	607.340	117.4	581.291	132.8
RSD	8.5×10^{-6}	1%	4.9×10^{-6}	2%	6.2×10^{-6}	1%	7.2×10^{-6}	2%	6.2×10^{-6}	2%

[a] Conditions: an 87 cm × 29.7 μm i.d. capillary packed with 3-μm porous C18-bonded particles equipped with a single ESI emitter (~5-μm orifice); 200-nL sample loop was used to introduce different concentrations of the yeast soluble protein tryptic digest sample to yield total mass loading amount from 25 to 1000 ng; peaks were randomly picked up across the elution time. Other conditions are the same as for Table 3. [b] $RSD_{m/z,\ total} = 6.4 \times 10^{-6}$; $RSD_{RT,\ total} = 2\%$. Calculations of $RSD_{m/z,\ total}$ and $RSD_{RT,\ total}$ exclude data from 25-ng run.

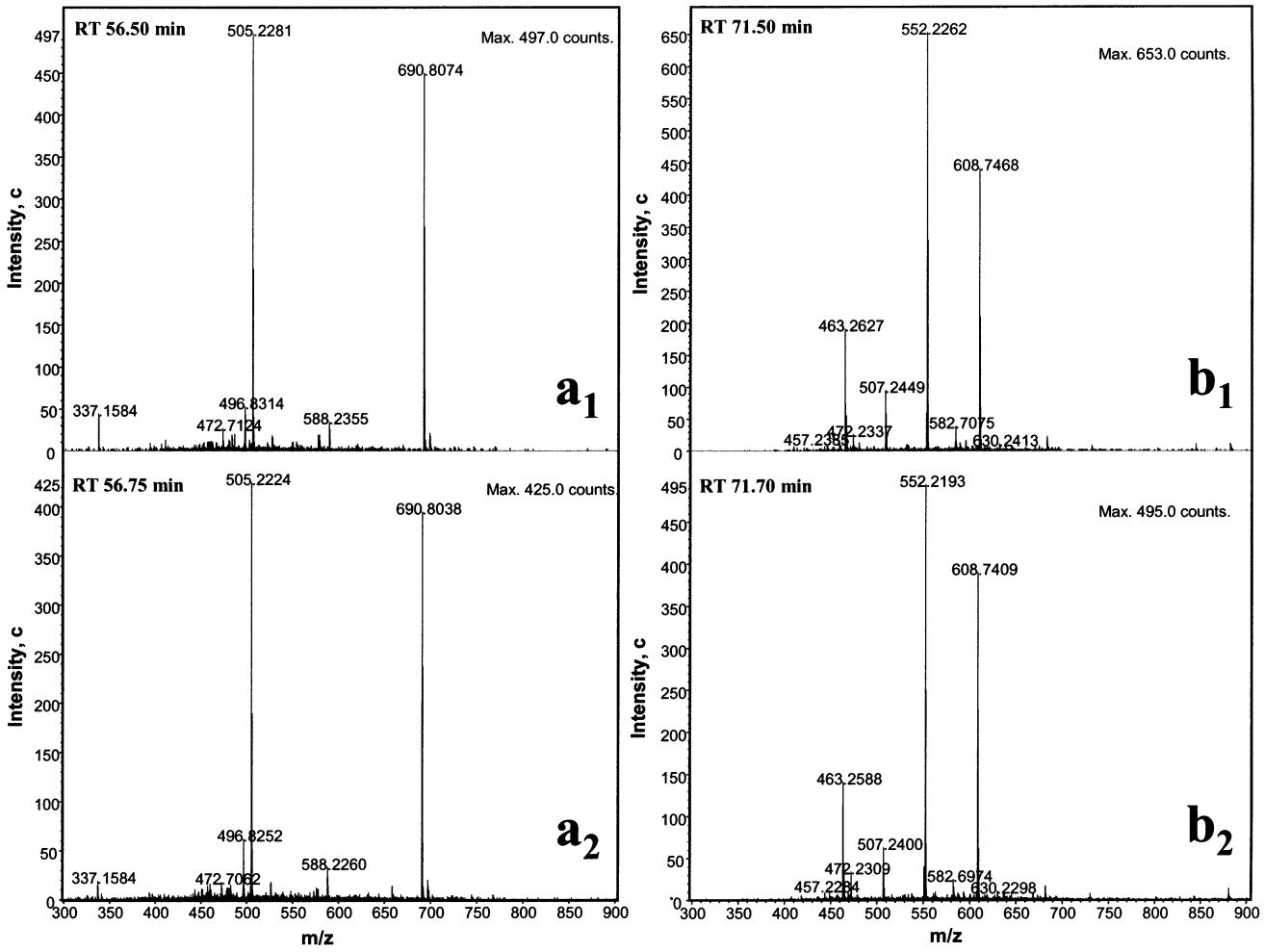

Figure 11. Reproducibility of mass spectra for corresponding chromatographic peaks in two nanoLC/nanoESI-MS analyses. Conditions are the same as in Figure 3.

(average RSD of 4.1 ppm; see Table 3); however, the chromatographic elution variance (the average RSD of 2%) was typically much larger than that for run-to-run studies (an average of RSD of 0.4%). The relatively large variance in chromatographic elution resulted from a slight systematic increase in elution times upon increasing the sample loadings from 50 to 500 ng. Using relative

Table 5. Reproducibility of Column to Column for High-Efficiency NanoLC/NanoESI-MS[a,b]

column	m/z	RT (min)	I (c)	m/z	RT (min)	I (c)	m/z	RT (min)	I (c)	m/z	RT (min)	I (c)	m/z	RT (min)	I (c)
1	356.237	32.54	684	541.311	41.29	1193	412.781	52.21	944	488.324	69.17	825	497.782	76.21	263
2	356.234	35.91	849	541.310	44.37	1933	412.780	57.63	1513	488.324	72.33	1376	497.785	79.29	452
3	356.233	34.21	937	541.314	42.54	1826	412.775	55.63	1231	488.322	70.54	1386	497.787	77.33	432
4	356.239	33.75	717	541.298	42.16	1781	412.778	55.88	1182	488.325	70.88	912	497.781	78.04	359
5	356.230	32.00	936	541.294	40.33	1055	412.772	52.79	936	488.314	67.33	816	497.774	73.83	391
av	356.235	33.68	824	541.305	42.14	1558	412.777	54.82	1161	488.322	70.05	1063	497.782	76.94	379
RSD	7.8×10^{-6}	3.3%	12%	13×10^{-6}	2.5%	22%	7.2×10^{-6}	3.4%	15%	6.1×10^{-6}	2.1%	24%	6.8×10^{-6}	2.0%	14%
1	509.834	83.34	683	576.379	100.7	2804	530.358	107.4	1367	543.683	120.0	268	581.387	128.7	616
2	509.834	86.91	970	576.378	102.8	3502	530.358	110.3	1854	543.689	122.5	336	581.387	131.0	890
3	509.834	84.91	906	576.377	100.4	3536	530.359	107.6	1739	543.688	119.9	312	581.387	128.3	772
4	509.824	85.58	776	576.370	101.4	2350	530.352	109.0	1300	543.686	121.0	268	581.379	129.5	529
5	509.829	81.50	814	576.365	96.91	2847	530.347	104.0	1527	543.679	116.8	274	581.373	124.9	751
av	509.831	84.45	830	576.374	100.4	3008	530.355	107.7	1557	543.685	120.0	292	581.386	128.5	711
RSD	7.1×10^{-6}	1.9%	14%	8.7×10^{-6}	1.4%	14%	7.9×10^{-6}	1.2%	12%	5.8×10^{-6}	1.1%	9.0%	7.9×10^{-6}	1.1%	16%

[a] Conditions: five 87 cm × 29.7 μm i.d. capillaries packed with 3-μm porous C18-bonded particles were used with equipment of individual ESI emitter (~5-μm-i.d. orifice) for each capillary column; the same sample (100 ng of a yeast soluble protein tryptic digest) was used for these five column runs under the same experimental conditions as for Table 3. [b] $RSD_{m/z,\ total} = 7.8 \times 10^{-6}$; $RSD_{RT,\ total} = 2.4\%$; $RSD_{I,\ total} = 15\%$.

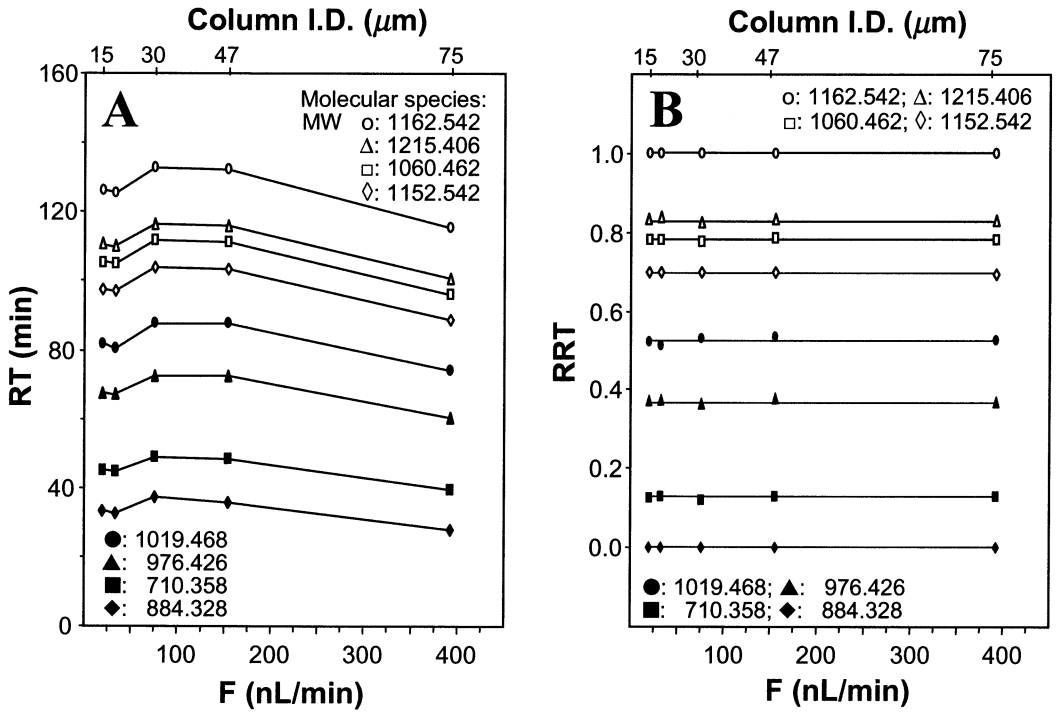

Figure 12. Chromatographic (A) absolute and (B) relative elution time reproducibility for individual components using various inner diameter packed capillaries and corresponding flow rates. RT, elution (retention) time; RRT, relative elution (retention) time. Conditions are the same as Figure 7.

chromatographic elution measurements (see discussion below), this average RSD can be decreased to <1%.

Table 5 gives the column-to-column reproducibility for five 87 cm × 29.7 μm i.d. packed capillaries. In these experiments, each packed capillary column used a different nanoESI tip. Examination of extracted ion chromatograms indicated that these capillaries yielded approximately the same separation efficiency and produced nanoLC/nanoESI-MS intensity with an average RSD of 15%, which is similar to what we observed for run to run on a single column and ESI emitter (average RSD of 14%; see Table 3). This suggests that packed capillaries and overall ESI performance can be quite reproducible. The variance of mass measurement accuracy (average RSD of 7.8 ppm) is slightly higher than that obtained for run to run on a single column (average RSD of 4.1 ppm; see Table 3), which was due to a systematic shift in the analysis of the last column tested (column 5). When mass accuracy was calibrated before each run, the mass measurement variance could routinely be controlled to within 5 ppm. The average RSD of chromatographic elution for the extracted species was 2.4%, which is larger than run-to-run variation. Using relative elution values, the RSD of chromatographic elution decreased to <1%.

Evaluation of the chromatographic elution reproducibility of packed capillaries with various inner diameters (from 14.9 to 74.5 μm) indicated that the elution time significantly depends on the column inner diameter, as illustrated in Figure 12A. Decreasing the inner diameter from 74.8 to 29.8 μm, the elution time increased

by ∼20% for less retained solutes. This shift likely resulted from a difference in the gradient delay for various inner diameter packed capillaries. The gradient delay, which is presently impractical to eliminate completely when splitlessly introducing sample with a switching valve, is determined by the void volume and mobile-phase flow through the separation capillary. With the gradient split tubing connected as illustrated in Figure 2, the void volume causing the gradient delay is ∼240 nL (including the sample loop). According to the mobile-phase flow rate listed in Table 1, the gradient delay time increased from 0.6 to 3.2 min as the capillary column inner diameters were decreased from 74.5 to 29.7 μm. This difference in delay time is responsible for the elution shift in Figure 12A. (For 14.9- and 19.8-μm-i.d. packed capillaries, we switched the injection valve back to the injection position after loading the sample on to the column and then started the gradient. This mode of operation minimizes the void volume to ∼40 nL and yields a delay of ∼2 min even for 14.8-μm-i.d. packed capillary column. This accounts for the decreased elution time for the 14.8- and 19.8-μm-i.d. packed capillaries compared to that on the 29.8-μm-i.d. packed capillary.) However, using relative chromatographic elution times, the average RSD was less than 1% for all runs. Figure 12B illustrates the relative chromatographic elution correlated with the first extracted peak elution time as 0 and the last as 1. The use of this relative elution approach allows correlation of chromatographic elution times under various conditions, including different columns and with different sample sizes.

CONCLUSIONS

Long (e.g., ∼87 cm) capillaries with inner diameters as small as 14.9 μm were successfully packed with 3-μm particles at 18 000 psi using carefully selected slurry solvents. NanoLC using these small inner diameter packed capillaries provided high-efficiency separations (peak capacities of $\sim 10^3$) for complex peptide mixtures in conjunction with nanoESI-MS detection conditions. NanoESI-MS signals responded linearly to sample loading over a defined range, but where greater detection sensitivity would also be beneficial to further extend the range over which highly quantitative results can be obtained. The number of detected components for a global yeast soluble protein digest (having individual peptide peak intensities of >40 counts/s) increased from 144 to 2037 as sample loading was increased from 25 to 1000 ng. In a flow rate range of 20−400 nL/min, nanoESI-MS responded linearly to the inverse of the mobile-phase flow rate, or approximately with the inverse square of the capillary column inner diameter. Decreasing the capillary column inner diameter from 74.5 to 14.9 μm increased the number of detected components having intensities of >40 counts/s (suitable for MS/MS and possible peptide identification) from 7 to 1345. The most sensitive analyses were achieved using a 14.9-μm-i.d. packed capillary column and a mobile-phase flow of ∼20 nL/min. For complex (proteomic) polypeptide mixtures, stationary phases having a pore size of 300 Å were sufficiently large to elute a wide range of components of interest. NanoLC elution time and nanoESI-MS response between runs were reproducible to <1 and <15%, respectively. Using normalized elution time values, elution variances were <1% for sample loadings from 25 to 1000 ng for either identical or different inner diameter columns (from 14.9 to 74.5 μm). Applications of these packed narrow capillaries coupled on-line with more sensitive FTICR instrumentation is now being investigated, and we project analysis of subnanogram proteomic samples should be possible.

ACKNOWLEDGMENT

We thank the U.S. Department of Energy, Office of Biological and Environmental Research, and the National Cancer Institute (Grants CA 86340 and CA 93306) for their support of portions of this research. Pacific Northwest National Laboratory is operated by the Battelle Memorial Institute for the U.S. Department of Energy through Contract DE-ACO6-76RLO 1830.

Received for review April 8, 2002. Accepted June 3, 2002.

AC0202280